Structural, Spectroscopic and Hirshfeld Surface Analysis of Anilinium Malonate

F. Mary Anjalin[1], N. Kanagathara[1,*], M.K. Marchewka[2] and T. Srinivasan[3]

[1]Department of Physics, Saveetha School of Engineering, Saveetha Institute of Medical and Technical Sciences, Thandalum, Chennai-602105, India

[2]Institute of Low Temperature and Structure Research, Polish Academy of Sciences, 50-950 Wroclaw, 2, P.O. Box 937, Poland

[3]Department of Physics with Computer Application, A.M. Jain College, Meenambakkam, Chennai-600114, India

*Corresponding author: E-mail: kanagathara23275@gmail.com

The comprehensive elucidation of the crystal structure, vibrational and Hirshfeld surface analysis of new crystalline product anilinium malonate $C_6H_5NH_3^+ \cdot C_3H_3O_4^-$ are presented in this communication. Single crystals of anilinium malonate have been grown by the method of slow evaporation at room temperature. Single crystal XRD study has been carried out to study the structural properties of the grown crystal and it reveals that the crystal crystallizes in the monoclinic system with centrosymmetric space group P2(1)/n. Room temperature powder infrared and Raman spectra of the aniline malonic acid molecular complex (1:1) were carried out. All the characteristic frequencies present in the crystal gives the notable vibrational effect. Hirshfeld surface analysis has been carried out to know the intercontact between the atoms in the structure of the grown crystal.

Keywords: Crystal structure, Vibrational studies, Hydrogen bond, Hirshfeld analysis.

INTRODUCTION

In recent years, organic materials with aromatic rings generally consist of a π-electron conjugated structure that exhibit significant nonlinear optical activity, which makes its wide applications in opto electronic and photonic applications [1]. Aniline is one such aromatic amine consists of a phenyl group attached to an amino group widely produced for a variety of industrial and commercial purposes, including dyestuff, pesticide and pharmaceuticals manufacturing. The derivatives of aniline usually form inter- or intra-molecular hydrogen bonding in solid state or with solvent in solutions due to its interesting polarity (electron donor) of amino group. Aniline and its derivatives have been widely used as starting materials for chemicals, pharmaceuticals, dyes, electro-optical, biological, materials science and many other industrial processes [2-4]. Many researchers have studied the properties of pure as well as doped aniline and its derivatives [5-9].

Carboxylic acid is an indispensable compound for living organism which has strong coordination with various transition metal ions such as Cu(II), Co(II), Ni(II) *etc*. and makes it applicability in many biological systems [10,11]. Two carboxylic group present in the malonic acid can act as chelating ligand form complex with transition metals may lead to fascinating structures [12,13]. Also this carboxylic group can act as a magnetic centre for coupling either ferromagnetic or antiferromagnetic materials [14]. The crystal structure of anilinium 3,4-dihydroxy benzoate, anilinium dihydrogen phosphate was reported earlier [15,16]. In the present communication, we have attempted to grow aniline with malonic acid (Fig. 1) and the grown crystals have been subjected to structural and spectroscopic characterization techniques. In addition to that we have carried out the Hirshfeld surface analysis to know the intercontact between the obtained crystalline products.

EXPERIMENTAL

High purity AR grade samples of aniline and malonic acid were taken in 1:1 molar ratio. At first, aniline was dissolved in double distilled water and the solution was allowed to stir well. To the clear solution of aniline, the dissolved malonic acid solution was added gently and stirred continuously for 6 h to

Fig. 1. Photograph of anilinium malonate

get the homogenous solution. Then the solution was filtered and allowed to evaporate at room temperature, which yielded whitish crystals within a period of 25-30 days (**Scheme-I**).
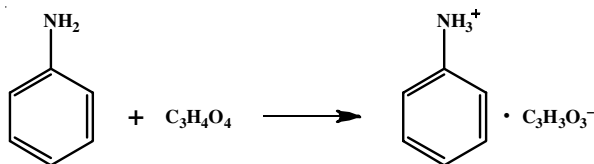
Scheme-I: Synthetic route of anilinium malonate compound

RESULTS AND DISCUSSION

X-ray data collection and structure description: Single crystal X-ray diffraction data of anilinium malonate were collected using KUMA KM-4 diffractometer of two-dimensional area CCD detector using graphite monochromatic MoK$_\alpha$ radiation (λ = 0.71073 Å) with ω scan [17]. Good quality anilinium malonate single crystal was used. The crystal structure was solved by a direct method with subsequent difference in Fourier syntheses of SHELXTL-PLUS program system [18] and SHELXL 97 is used for the structure refinement [19]. Successive refinements based on F^2 lead to a reliability factor of R = 0.066. Anisotropic displacement parameters were included for all non hydrogen atoms. The ORTEP representation of the molecule with 30 % probability ellipsoids for non-hydrogen atoms and the packing of the molecule in unit cell of the crystal are depicted in Figs. 2 and 3, respectively. Fig. 4 represents the molecular packing of the anilinium malonate forming two dimensional networks. Figs. 5 and 6 show only the hydrogen bond interactions formed in the grown crystal and malonic acid molecules. Fig. 7 shows the chains of malonate anions running along crystallographic Y direction formed through O14-H10···O15a and O19-H13···O17f hydrogen bonds. Fig. 8 represents the chains of malonate anions running along crystallographic Y direction formed through O12-H7···O21d, O24-H16···O10, O6-H4···O3 and O1-H1···O7c hydrogen bonds.

Single crystal X-ray diffraction data reveals that the grown anilinium malonate crystal crystallizes in monoclinic crystal system with centrosymmetric space group P2(1)/n. The lattice parameters are calculated to be a = 14.203(3) Å, b = 9.220(2) Å, c = 21.294(4) Å, α = γ = 90° and β = 95.59(3)°. The volume of the unit cell is calculated to be = 1404.0(4) (Å)^3. The asymmetric unit of anilinium malonate consists of six anilinium cation and six malonate anion with unit cell contains 12 molecules. In the independent part of the elementary cell there are six crystallographically independent aniline cations and malonate anions. In the aniline malonate crystal in the elemental cell there are six crystallographically non-covalent

Fig. 2. ORTEP plot of anilinium malonate with the atom numbering (Scheme. Displacement ellipsoids are drawn at 30 % probability level)
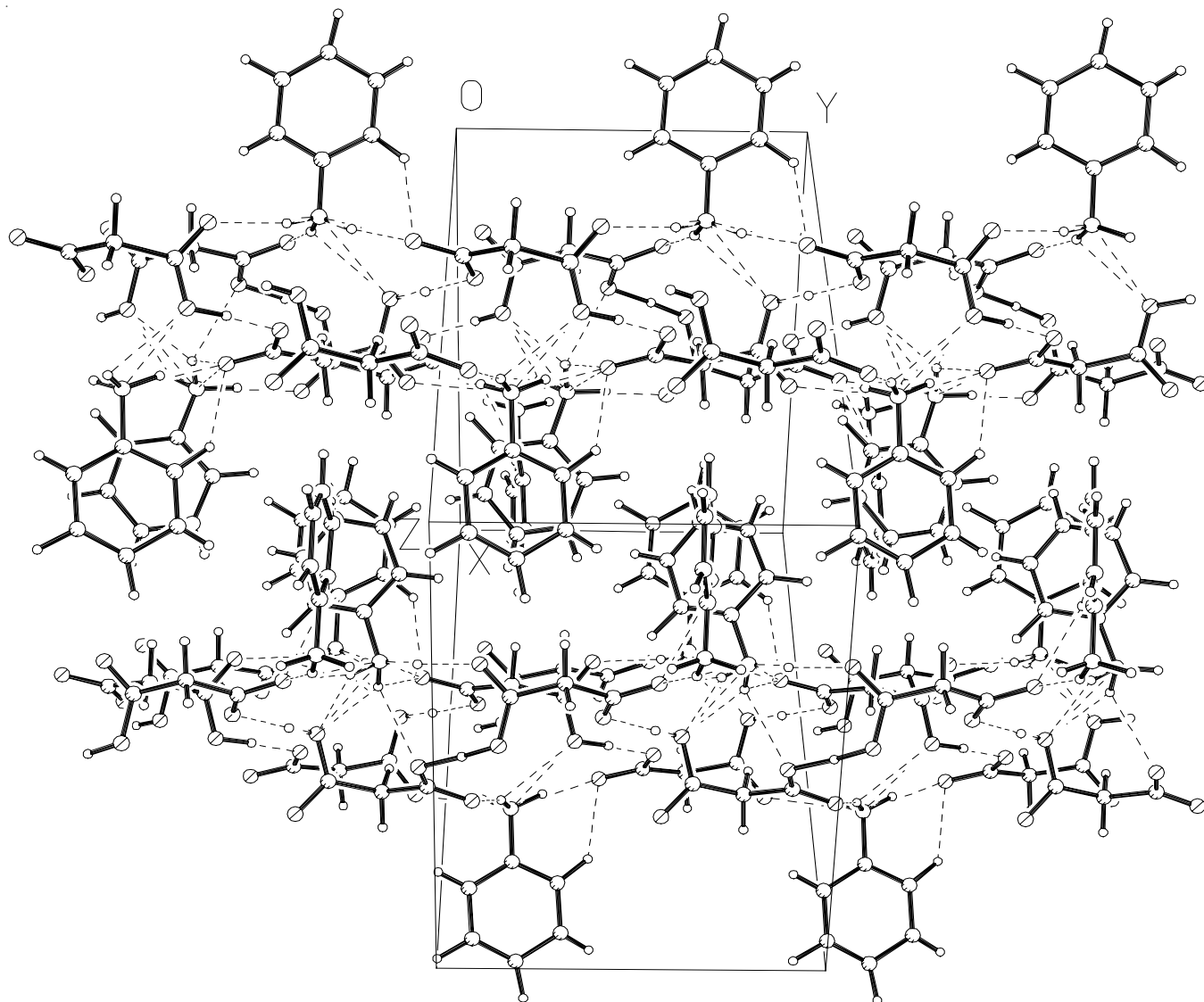
Fig. 3. Packing of the molecules in elementary unit cell for anilinium malonate
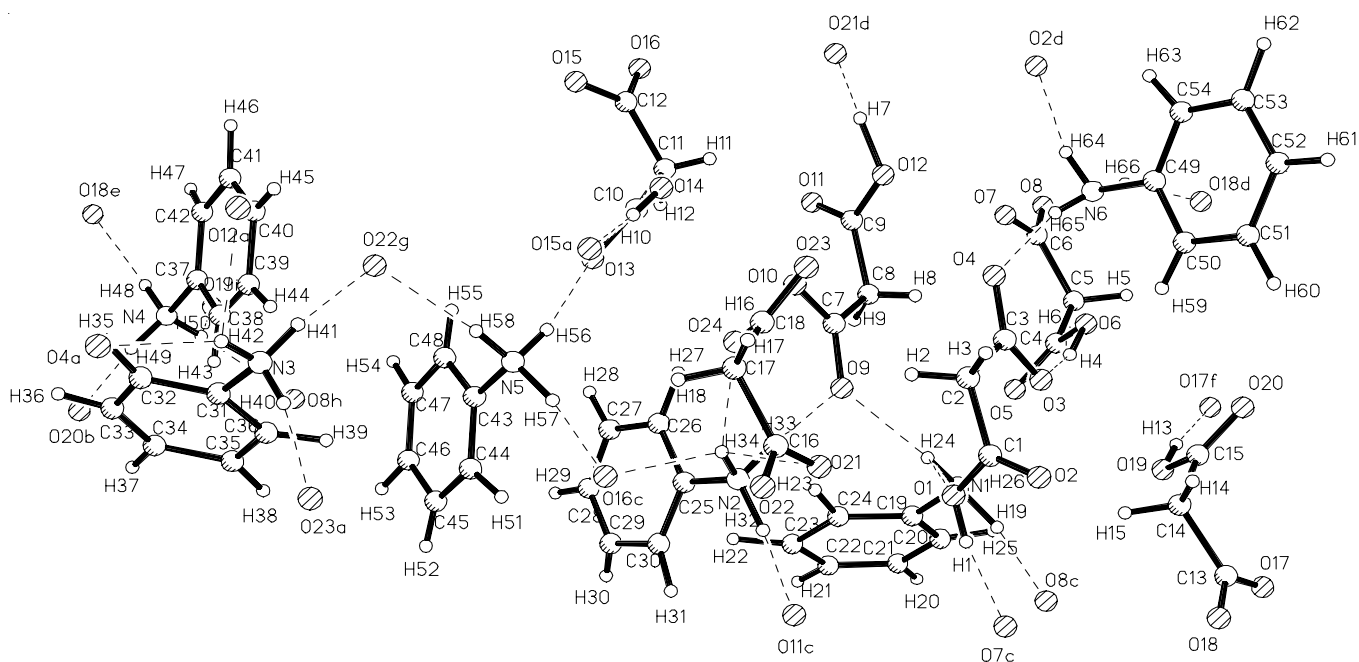
Fig. 4. Molecular packing of anilinium malonate forming two dimensional networks
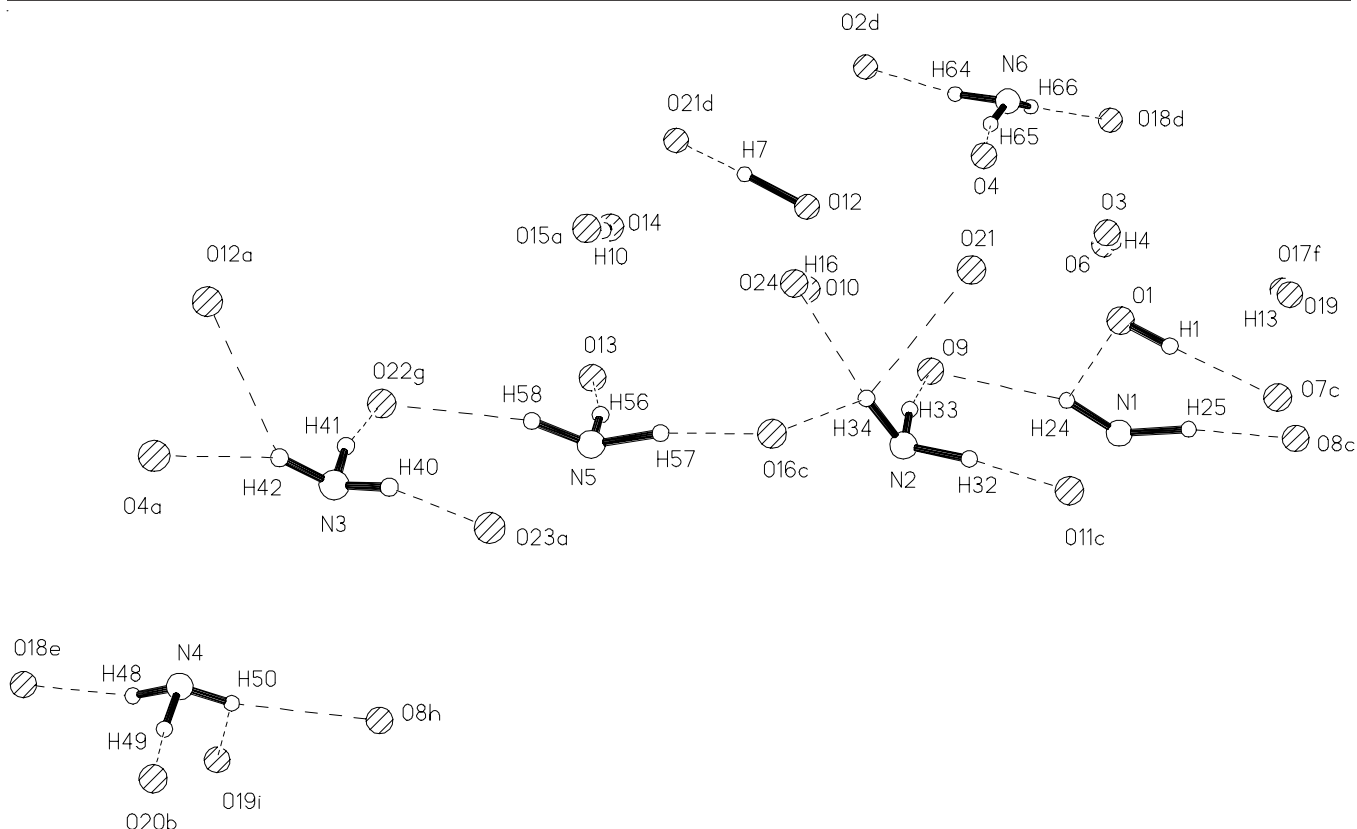
Fig. 5. Hydrogen bonds system formed in anilinium malonate. Only the atoms participated in hydrogen bonds are shown for clarity
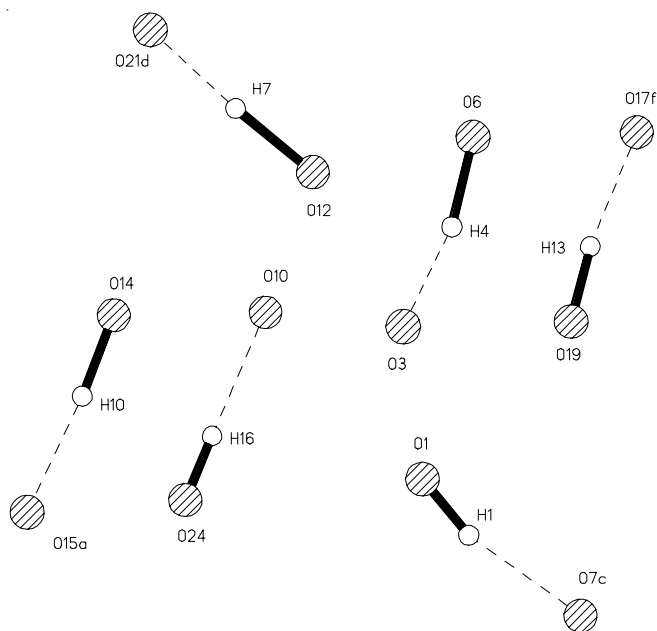
Fig. 6. Hydrogen bonds formed between malonic acid molecules

cations of protonated aniline. Only some of them participate in unconventional hydrogen bonds type C-H···π interaction. The structure is stabilized by hydrogen bonds, where the proton donors are the nitrogen atoms of the amino groups and the proton acceptors are oxygen atoms of carboxylate group's *i.e.* an intramolecular O-H···O hydrogen bond occurs in each anion. In the crystal, O-H···O and N-H···O hydrogen bonds link the cations and anions into a three dimensional array. The structure is further consolidated by weak C-H···O interactions.

In aniline cation, all the H atoms attached to the C atoms were positioned geometrically with C-H bond length of 0.920 Å whereas C-H bond length in malonate anion is 0.961 Å. It indicates the C-H bond length of aniline is lesser than malonic acid molecule. In turn C-O bond lengths of malonic acid falls into 4 classes *viz.* 1.243, 1.269, 1.221 and 1.307 Å which clearly indicates that the bond length of C-O (C1-O1) in carboxyl group where protonation occurs have increased bond length of 1.307 Å. All O-C-O angles of malonate anion have the bond angle of about 123°. The hydrogen atom in carboxyl group of malonaic acid protonated with aniline molecule carry the bond angle of 129.35° whereas the other hydrogen atom carboxyl group have the bond angle of 114.84°. All these parameters confirm the occurrence of protonation between the aniline and malonic acid molecules. The geometric parameters of the anilinium as well as malonate molecule are comparable with those determined by earlier researcher [15,16,20]. Table-1 provides the crystal data and structure refinement parameters of the anilinium malonate. Interatomic distances and angles values in aniline cations and malonate anions are standard for these molecules. The geometric parameters of hydrogen bonds formed in the anilinium malonate crystal are shown in Table-2 with symmetry codes. Selected bond distances and bond angles are compiled in Table-3. Atomic displacement parameters, fractional atomic coordinates and isotropic or equivalent isotropic displacement parameters (Å^2) are listed in Tables 4 and 5.

Powder X-ray diffraction studies: MERCURY 3.8 [21] software tool was used to investigate and analyze the crystal structure. By giving crystallographic information file as the
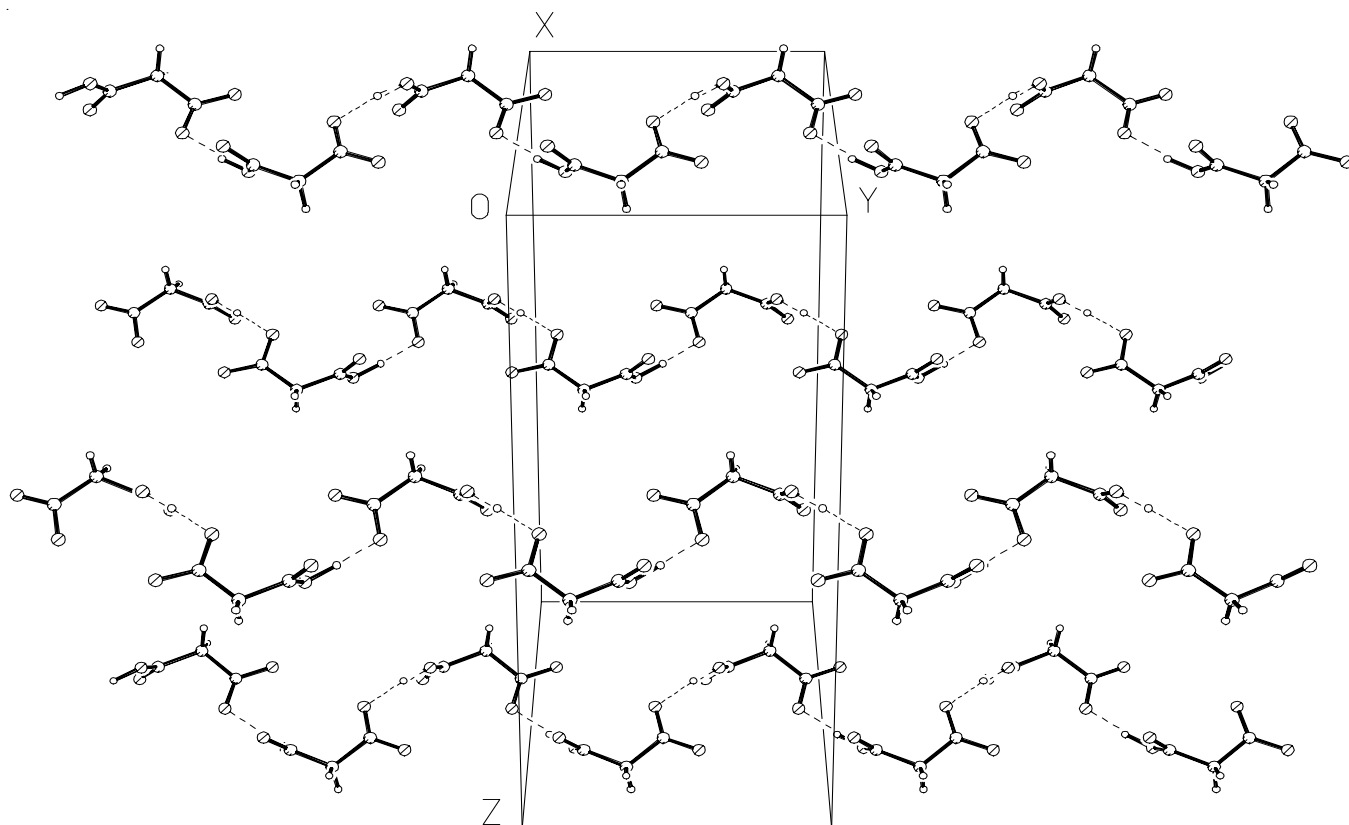
Fig. 7. Chains of malonate anions running along crystallographic Y direction formed through O14-H10···O15a and O19-H13···O17f hydrogen bonds
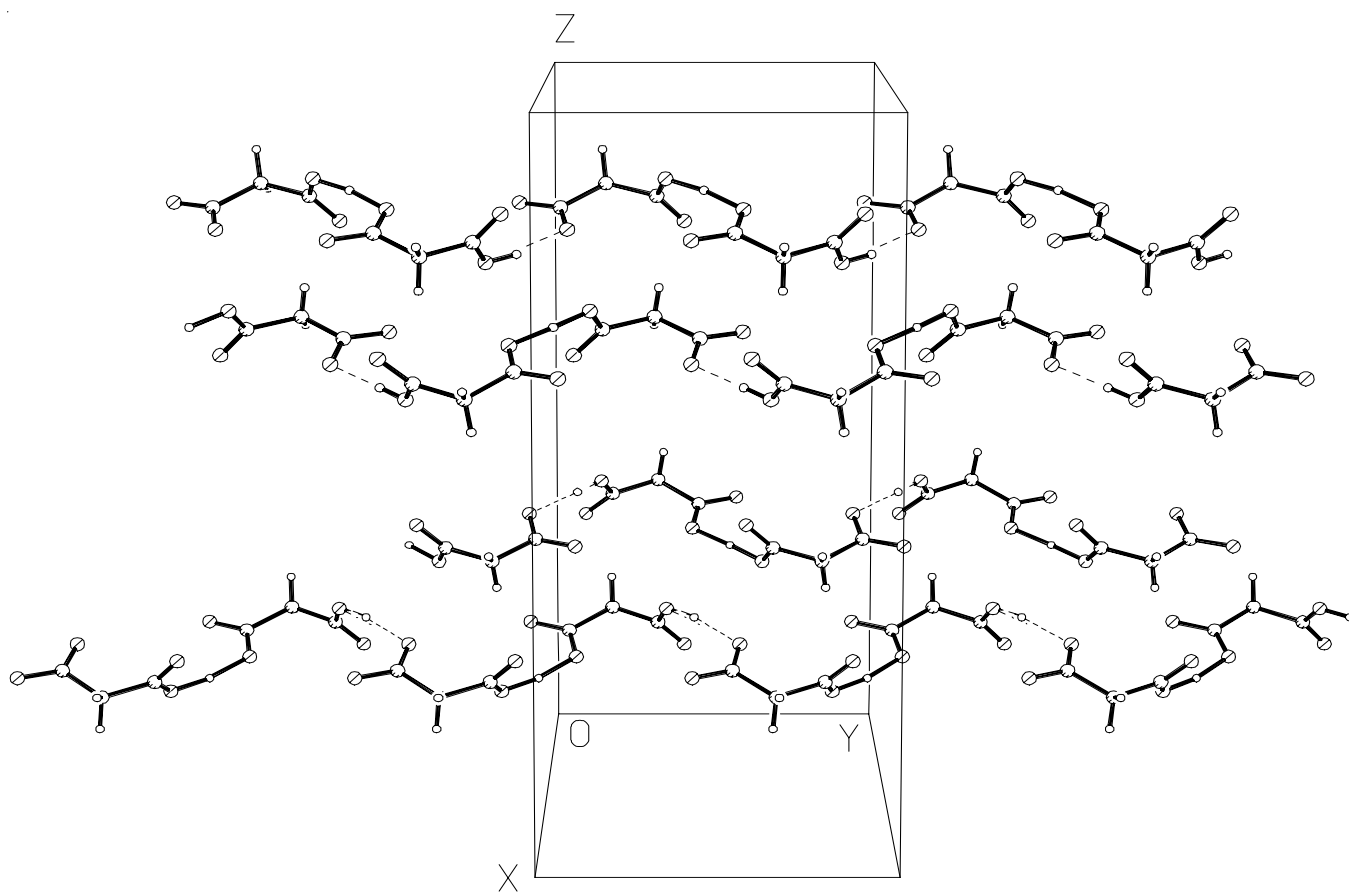
Fig. 8. Chains of malonate anions running along crystallographic Y direction formed through O12-H7···O21d, O24-H16···O10, O6-H4···O3 and O1-H1···O7c hydrogen bonds

TABLE-1 CRYSTAL DATA AND STRUCTURE REFINEMENT FOR ANILINIUM MALONATE	
Empirical formula	$C_9H_{11}NO_4$
Formula weight (g mol^{-1})	197.19
Temperature (K)	293(2)
Wavelength (A)	0.71073 Å
Crystal system	Monoclinic
Space group	P2(1)/n
a	14.203(3)Å
b	9.220(2)Å
c	21.294(4) Å
α	90°
β	95.59(3)°
γ	90°
V	2775.2(10) (Å)^3
Z	12
D_{calc} (Mg m^{-3})	1.416
Absorption coefficient (mm^{-1})	0.112
F(000)	1248
Crystal size (mm)	0.36 x 0.28 x 0.24
Theta range for data collection (°)	4.24-46.23
Index ranges	h =--17 → 18; k =-18→12; l =-42→25
Completeness to θ	100 %
Refinement method	Full-matrix least squares on F^2
Data/restraints/parameters	10639/0/392
Goodness of fit on F^2	0.942
Extinction coefficient	0.0099(3)
Largest differences peak and hole (e.Å^{-3})	0.17 and-0.20

input powder X-ray diffraction pattern of the grown crystal can be generated which would be used to identify the crystalline nature of the grown crystal. Fig. 9 depicts the generated powder X-ray diffraction pattern of anilinium malonate. The results of the powder X-ray diffraction are analyzed with the help of Mercury 3.8 software. Debye-Scherrer's formula is used to determine the crystallite size (D) which is given as

$$D = \frac{K\lambda}{(\beta_{1/2} \cos\theta)} \quad (1)$$

where K = 0.89; λ = 1.5405 Å and $\beta_{1/2}$ is the peak width of the reflection at half intensity. The maximum intensity peak occurs at 2θ = 22°. The average value of the crystallite size of anilinium malonate is found to be 13.962 μm.
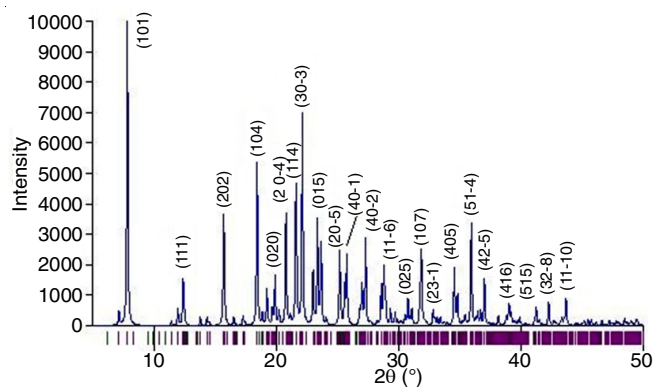
Fig. 9. Simulated powder X-ray diffraction pattern of anilinium malonate

Vibrational spectroscopic analysis: The Raman and infrared spectra of the grown crystal have been carried out to identify the functional groups present in the sample. An infrared spectroscopy is an excellent tool for the investigation of

TABLE-2 HYDROGEN BOND GEOMETRY (Å, °)				
D–H···A	Distance (Å)			Angle (°)
	D–H	H···A	D···A	D···A
O4F–H4FC···O2C	0.978(7)	1.550(7)	2.5233(10)	173.0(6)
O2B–H2BA···O3A	1.010(10)	1.529(11)	2.5259(9)	167.9(13)
O2D–H2DD···O3D^{ii}	0.993(8)	1.535(8)	2.5270(9)	177.8(8)
O3E–H3EE···O1E^{vii}	0.989(8)	1.556(8)	2.5415(10)	174.0(9)
O4C–H4CF···O1F^{vi}	1.018(8)	1.524(8)	2.5417(9)	178.0(8)
O1A–H1AB···O3B^{viii}	0.968(7)	1.648(8)	2.5836(9)	161.3(8)
N1I–H11I···O3F^{ii}	0.928(6)	1.822(6)	2.7329(11)	166.3(6)
N1J–H12J···O4E^{iv}	0.915(7)	1.885(7)	2.7693(11)	162.1(6)
N1H–H11H···O3C^{i}	0.991(8)	1.788(8)	2.7749(11)	173.5(8)
N1G–H13G···O1B	0.973(8)	1.889(8)	2.7850(11)	151.9(7)
N1K–H11K···O1D	0.928(8)	1.902(8)	2.8046(11)	163.5(7)
N1G–H12G···O4B^{i}	0.997(8)	1.838(8)	2.8166(11)	166.5(7)
N1L–H11L···O2A^{vi}	0.952(7)	1.888(7)	2.8232(11)	167.0(6)
N1H–H13H···O4F	0.942(6)	2.109(7)	2.8341(10)	132.8(6)
N1I–H12I···O2F^{iii}	0.958(7)	1.910(7)	2.8510(11)	166.8(7)
N1L–H12L···O4A	0.923(9)	2.021(9)	2.8946(11)	157.3(8)
N1K–H12K···O4D^{i}	1.020(7)	1.901(7)	2.9081(11)	168.7(6)
N1H–H13H···O4D^{i}	0.942(6)	2.303(7)	2.9209(12)	122.6(5)
N1L–H13L···O2E^{vi}	0.980(7)	1.971(7)	2.9264(13)	164.1(6)
N1H–H12H···O1C	0.911(8)	2.052(8)	2.9339(11)	162.5(8)
N1I–H13I···O4C^{ii}	0.937(7)	2.402(8)	2.9796(10)	119.7(7)
N1G–H11G···O1A	0.968(8)	2.502(9)	2.9949(10)	111.5(7)
N1J–H13J···O4B^{v}	0.906(8)	2.236(9)	3.0208(12)	144.7(8)
N1K–H13K···O2F^{iii}	0.940(8)	2.103(8)	3.0223(13)	165.4(7)

Symmetry codes: (i) x,1+y,z; (ii) 2-x,1/2+y,1-z; (iii) 2-x,-1/2+y,1-z; (iv) x,y,-1+z; (v) 1-x,-1/2+y,1-z; (vi) 1-x,1/2+y,1-z; (vii) x,-1+y,z; (viii) 1-x,-1/2+y,2-z

		TABLE-3			
		SELECTED BOND DISTANCES (Å) AND BOND ANGLES (°) OF ANILINIUM MALONATE			
Atom	Bond distance (Å)	Atom	Bond distance (Å)	Atom	Bond distance (Å)
O1A-C1A	1.309	N1D-H1D1	0.920	C6E-C5E	1.3822
O1A-HO1A	0.982	N1D-H1D2	0.920	C6E-H6E	0.9200
O3A-C3A	1.273	N1D-H1D3	0.920	C5E-H5E	0.9200
O4A-C3A	1.247	C1D-C6D	1.375	N1F-C1F	1.4525
O2A-C1A	1.223	C1D-C2D	1.368	N1F-H1F1	0.9200
C1A-C2A	1.499	C6D-C5D	1.384	N1F-H1F2	0.9200
C3A-C2A	1.524	C6D-H6D	0.920	N1F-H1F3	0.9200
C2A-H2A1	0.960	C4D-C5D	1.371	C1F-C2F	1.3707
C2A-H2A2	0.960	C4D-C3D	1.376	C1F-C6F	1.3743
O1B-C1B	1.259	C4D-H4D	0.920	C1F-N1F	1.453
O3B-C3B	1.301	C5D-H5D	0.920	C6F-C1F	1.374
O3B-H03B	0.995	C2D-C3D	1.383	C6F-C5F	1.391
O4B-C3B	1.221	C2D-H2D	0.920	C6F-H6F	0.920
O2B-C1B	1.254	C3D-H3D	0.920	C3F-C4F	1.365
C3B-C2B	1.504	N1E-C1E	1.468	C3F-C2F	1.384
C1B-C2B	1.529	N1E-H1E1	0.920	C3F-H3F	0.920
C2B-H2B1	0.960	N1E-H1E2	0.920	C5F-C4F	1.371
C2B-H2B2	0.960	N1E-H1E3	0.920	C5F-C6F	1.390
O1C-C1C	1.307	C1E-C6E	1.376	C5F-H5F	0.920
O1C-HO1C	0.985	C1E-C2E	1.382	C4F-H4F	0.920
O3C-C3C	1.268	C2E-C3E	1.378	C2F-C1F	1.370
O4C-C3C	1.243	C2E-H2E	0.920	C2F-C3F	1.384
O2C-C1C	1.221	C4E-C5E	1.369	C2F-H2F	0.920
C1C-C2C	1.505	C4E-C3E	1.373		
C3C-C2C	1.521	C4E-H4E	0.920		
C2C-H2C1	0.960	C3E-H3E	0.920		
C2C-H2C2	0.960	N1D-C1D	1.468		
Atom	Bond angle (°)	Atom	Bond angle (°)	Atom	Bond angle (°)
C1A-O1A-HO1A	114.4	C3C-C2C-H2C1	108.7	C3E-C2E-H2E	120.4
O2A-C1A-O1A	123.7	C1C-C2C-H2C2	108.7	C1E-C2E-H2E	120.4
O2A-C1A-C2A	121.9	C3C-C2C-H2C2	108.7	C5E-C4E-C3E	120.1
O1A-C1A-C2A	114.4	H2C1-C2C-H2C2	107.6	C5E-C4E-H4E	120.0
O4A-C3A-O3A	124.6	C1D-N1D-H1D1	109.5	C3E-C4E-H4E	120.0
O4A-C3A-C2A	117.9	C1D-N1D-H1D2	109.5	C4E-C3E-C2E	120.4
O3A-C3A-C2A	117.3	H1D1-N1D-H1D2	109.5	C4E-C3E-H3E	119.8
C1A-C2A-C3A	114.3	H1D1-N1D-H1D3	109.5	C2E-C3E-H3E	119.8
C1A-C2A-H2A1	108.7	C6D-C1D-C2D	120.9	C1E-C6E-C5E	119.1
C3A-C2A-H2A1	108.7	C6D-C1D-N1D	119.8	C1E-C6E-H6E	120.4
C1A-C2A-H2A2	108.7	C2D-C1D-N1D	119.2	C5E-C6E-H6E	120.4
C3A-C2A-H2A2	108.7	C1D-C6D-C5D	119.2	C4E-C5E-C6E	120.5
H2A1-C2A-H2A2	107.6	C5D-C6D-H6D	120.4	C4E-C5E-H5E	119.8
C3B-O3B-H03B	115.1	C5D-C4D-C3D	120.2	C6E-C5E-H5E	119.8
O4B-C3B-O3B	123.7	C5D-C4D-H4D	119.9	C1F-N1F-H1F1	109.5
O4B-C3B-C2B	121.6	C3D-C4D-H4D	119.9	C1F-N1F-H1F2	109.5
O3B-C3B-C2B	114.6	C4D-C5D-C6D	120.2	H1F1-N1F-H1F2	109.5
O2B-C1B-O1B	125.1	C4D-C5D-H5D	119.9	C1F-N1F-H1F3	109.5
O2B-C1B-C2B	116.8	C6D-C5D-H5D	119.9	H1F1-N1F-H1F3	109.5
O1B-C1B-C2B	117.9	C1D-C2D-C3D	119.6	H1F2-N1F-H1F3	109.5
C3B-C2B-C1B	114.9	C1D-C2D-H2D	120.2	C2F-C1F-C6F	121.2
C3B-C2B-H2B1	108.5	C3D-C2D-H2D	120.2	C2F-C1F-N1F	119.8
C1B-C2B-H2B1	108.5	C4D-C3D-C2D	119.6	C6F-C1F-N1F	118.9
C3B-C2B-H2B2	108.5	C4D-C3D-H3D	120.2	C1F-C6F-C5F	118.7
C1B-C2B-H2B2	108.5	C2D-C3D-H3D	120.2	C1F-C6F-H6F	120.6
H2B1-C2B-H2B2	107.5	C1E-N1E-H1E1	109.5	C5F-C6F-H6F	120.6
C1C-O1C-HO1C	114.8	C1E-N1E-H1E2	109.5	C4F-C3F-C2F	120.4
O2C-C1C-O1C	123.7	H1E1-N1E-H1E2	109.5	C4F-C3F-H3F	119.8
O2C-C1C-C2C	121.9	C1E-N1E-H1E3	109.5	C2F-C3F-H3F	119.8
O1C-C1C-C2C	114.2	H1E1-N1E-H1E3	109.5	C4F-C5F-C6F	120.4
O4C-C3C-O3C	124.5	H1E2-N1E-H1E3	109.5	C4F-C5F-H5F	119.8
O4C-C3C-C2C	118.2	C6E-C1E-C2E	120.7	C6F-C5F-H5F	119.8
O3C-C3C-C2C	117.2	C6E-C1E-N1E	120.7	C3F-C4F-C5F	120.0
C1C-C2C-C3C	114.1	C2E-C1E-N1E	118.5	C3F-C4F-H4F	120.0
C1C-C2C-H2C1	108.7	C3E-C2E-C1E	119.2	C5F-C4F-H4F	120.0

TABLE-4
ATOMIC DISPLACEMENT PARAMETERS (Å^2)

Atom	U11	U22	U33	U23	U13	U12
O1A	0.0362(4)	0.0272(4)	0.0481(5)	0.0036(4)	0.0002(4)	0.0024(4)
O3A	0.0363(4)	0.0295(4)	0.0509(5)	0.0001(4)	0.0139(4)	0.0004(4)
O4A	0.0471(5)	0.0265(4)	0.0484(5)	0.0007(4)	0.0052(4)	0.0068(4)
O2A	0.0491(5)	0.0343(5)	0.0503(5)	-0.0114(4)	-0.0050(4)	0.0015(4)
C1A	0.0324(6)	0.0249(6)	0.0353(6)	0.0003(5)	0.0083(5)	-0.0038(5)
C3A	0.0345(6)	0.0268(6)	0.0302(6)	-0.0038(5)	-0.0025(5)	0.0009(5)
C2A	0.0313(6)	0.0302(6)	0.0381(6)	-0.0029(5)	0.0073(5)	-0.0009(5)
O1B	0.0368(4)	0.0301(4)	0.0547(5)	-0.0011(4)	0.0134(4)	0.0003(4)
O3B	0.0341(4)	0.0276(4)	0.0540(5)	0.0024(4)	-0.0042(4)	-0.0020(4)
O4B	0.0533(5)	0.0313(5)	0.0540(5)	0.0114(4)	-0.0141(4)	-0.0041(4)
O2B	0.0422(5)	0.0261(4)	0.0594(6)	-0.0026(4)	0.0051(4)	-0.0057(4)
C3B	0.0325(6)	0.0249(6)	0.0339(6)	-0.0045(5)	0.0061(5)	0.0032(5)
C1B	0.0305(6)	0.0244(6)	0.0315(6)	0.0023(5)	-0.0041(5)	0.0016(5)
C2B	0.0308(6)	0.0245(6)	0.0386(6)	0.0012(5)	0.0063(5)	0.0005(5)
O1C	0.0364(4)	0.0282(4)	0.0498(5)	-0.0045(4)	0.0025(4)	0.0021(4)
O3C	0.0473(5)	0.0292(4)	0.0614(6)	0.0001(4)	0.0235(4)	-0.0019(4)
O4C	0.0479(5)	0.0279(4)	0.0545(5)	0.0036(4)	0.0065(4)	0.0082(4)
O2C	0.0534(5)	0.0327(5)	0.0464(5)	-0.0104(4)	-0.0054(4)	-0.0020(4)
C1C	0.0344(6)	0.0264(6)	0.0317(6)	0.0008(5)	0.0096(5)	-0.0053(5)
C3C	0.0315(6)	0.0284(6)	0.0323(6)	-0.0014(5)	-0.0043(5)	-0.0018(5)
C2C	0.0315(6)	0.0285(6)	0.0360(6)	-0.0006(5)	0.0057(5)	-0.0005(5)
N1D	0.0342(5)	0.0356(6)	0.0582(7)	-0.0140(5)	-0.0043(5)	0.0032(5)
C1D	0.0309(6)	0.0303(6)	0.0357(6)	-0.0065(5)	0.0038(5)	-0.0004(5)
C6D	0.0434(7)	0.0283(6)	0.0410(7)	-0.0026(6)	0.0023(6)	0.0004(6)
C4D	0.0444(7)	0.0517(8)	0.0361(7)	-0.0048(6)	-0.0057(6)	-0.0019(7)
C5D	0.0473(7)	0.0355(7)	0.0471(8)	-0.0090(6)	0.0002(6)	-0.0103(6)
C2D	0.0424(7)	0.0308(7)	0.0567(8)	0.0038(6)	0.0046(6)	-0.0070(6)
C3D	0.0552(8)	0.0431(8)	0.0465(8)	0.0114(7)	0.0010(7)	0.0032(7)
N1E	0.0369(5)	0.0311(5)	0.0536(6)	-0.0064(5)	-0.0054(5)	0.0033(5)
C1E	0.0342(6)	0.0245(6)	0.0399(7)	-0.0021(5)	-0.0019(5)	-0.0034(5)
C2E	0.0408(7)	0.0403(7)	0.0356(7)	0.0027(6)	0.0039(6)	-0.0015(6)
C4E	0.0593(8)	0.0410(7)	0.0532(8)	0.0044(7)	-0.0189(7)	-0.0107(7)
C3E	0.0360(7)	0.0480(8)	0.0611(9)	0.0103(7)	-0.0008(6)	-0.0057(6)
C6E	0.0474(8)	0.0508(8)	0.0505(8)	-0.0089(7)	0.0151(6)	0.0004(7)
C5E	0.0829(10)	0.0578(9)	0.0323(7)	-0.0093(7)	0.0010(7)	-0.0063(8)
N1F	0.0400(6)	0.0367(6)	0.0550(6)	-0.0128(5)	-0.0070(5)	0.0075(5)
C1F	0.0307(6)	0.0362(7)	0.0351(6)	0.0028(6)	0.0026(5)	0.0051(5)
C6F	0.0436(7)	0.0333(7)	0.0446(7)	-0.0008(6)	0.0069(6)	-0.0031(6)
C3F	0.0425(7)	0.0766(10)	0.0468(8)	0.0011(8)	-0.0027(6)	-0.0093(8)
C5F	0.0650(9)	0.0449(8)	0.0424(8)	0.0098(6)	0.0133(7)	0.0210(7)
C4F	0.0446(7)	0.0799(10)	0.0356(7)	0.0022(7)	-0.0005(6)	0.0186(8)
C2F	0.0442(7)	0.0496(8)	0.0465(8)	-0.0079(7)	0.0018(6)	0.0089(7)

the hydrogen bonds in the crystal. Thus, the vibrational spectra can be helpful in the elucidation of the role of such a kind of interaction in the structure of the crystals exhibiting nonlinear optical properties. The vibrational measurements were carried out at room temperature. Infrared spectra were taken with a Bruker IFS-88 spectrometer in the region 4000-80 cm^{-1}. The resolution was set up to 2 cm^{-1}, signal/noise ratio was established by 32 scans, weak apodisation. Powder Fourier transform Raman (FT Raman) spectra were taken with an FRA-106 attachment to the Bruker IFS-88 spectrometer equipped with Ge detector cooled to liquid nitrogen temperature. Nd^{3+}:YAG air-cooled diode pumped laser of power about 200 mW was used as an exciting source. The incident laser excitation is 1064 nm. The scattered light was collected at the angle of 180° in the region 3600-80 cm^{-1}, resolution 2 cm^{-1}, 256 scans. The measured spectra are shown in Figs. 10 and 11. The wavenumbers of the bands and their relative intensities for infrared absorption and Raman scattering experiments are provided in
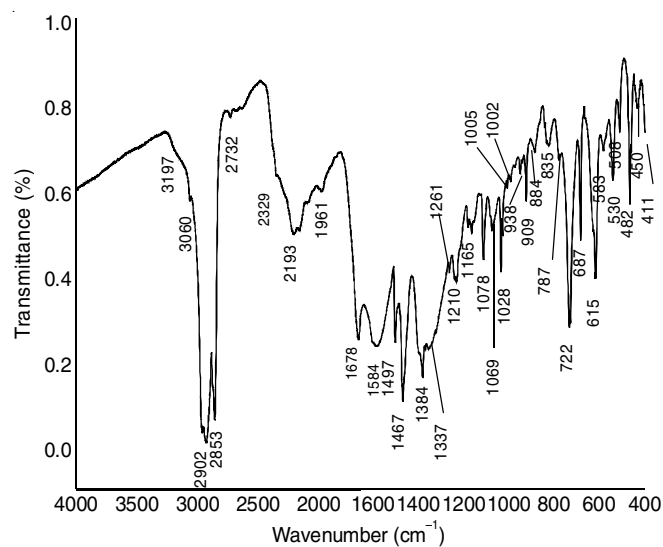
Fig. 10. FT-IR spectra of as grown anilinium malonate crystal

TABLE-5
FRACTIONAL ATOMIC COORDINATES AND ISOTROPIC OR EQUIVALENT ISOTROPIC DISPLACEMENT PARAMETERS (Å^2)

Atom	X	Y	z	U iso or equi	Atom	X	Y	Z	U iso or equi
O1A	0.0403	0.1482	0.9721	0.0375	C2D	0.4940	0.05977	0.8976	0.0433
O3A	0.0467	0.4263	0.9015	0.0383	H2D	0.4602	-0.0252	0.8926	0.0500
O4A	-0.0656	0.5733	0.9313	0.0406	C3D	0.5741	0.0669	0.9401	0.0485
O2A	-0.0748	0.0948	0.8966	0.0452	H3D	0.5941	-0.0135	0.9632	0.0500
C1A	-0.0385	0.1768	0.9371	0.0305	N1E	0.7193	0.1787	0.4836	0.0412
C3A	-0.0298	0.4509	0.9261	0.0309	H1E1	0.6640	0.1697	0.5025	0.0500
C2A	-0.0816	0.3207	0.9504	0.0330	H1E2	0.7259	0.1005	0.4576	0.0500
H2A1	-0.0830	0.3306	0.9953	0.0500	H1E3	0.7177	0.2628	0.4603	0.0500
H2A2	-0.1459	0.3219	0.9317	0.050	C1E	0.7997	0.1837	0.5324	0.0332
O1B	0.8671	0.0721	0.0621	0.0399	C2E	0.8901	0.1692	0.5142	0.0389
O3B	0.8647	0.3542	0.1325	0.0392	H2E	0.8993	0.1575	0.4724	0.0500
O4B	0.7432	0.4078	0.0626	0.0475	C4E	0.9524	0.1910	0.6220	0.0527
O2B	0.7506	-0.0706	0.0889	0.0426	H4E	1.0036	0.1938	0.6521	0.0500
C3B	0.7839	0.3252	0.1009	0.0302	C3E	0.9662	0.1728	0.5596	0.0487
C1B	0.7906	0.0501	0.0859	0.0293	H3E	1.0266	0.1629	0.5480	0.050
C2B	0.7432	0.1795	0.1150	0.0311	C6E	0.7853	0.2005	0.5950	0.0489
H2B1	0.6772	0.1793	0.1000	0.0500	H6E	0.7251	0.2086	0.6070	0.0500
H2B2	0.7479	0.1668	0.1600	0.0500	C5E	0.8627	0.2049	0.6396	0.0580
O1C	0.7121	0.1465	0.3097	0.0383	H5E	0.8539	0.2173	0.6816	0.0500
O3C	0.7089	0.4232	0.2305	0.0448	N1F	1.0281	0.1790	0.1479	0.0447
O4C	0.6032	0.5742	0.2650	0.0433	H1F1	0.9674	0.1729	0.1594	0.0500
O2C	0.5918	0.0998	0.2374	0.0449	H1F2	1.0465	0.0900	0.1340	0.0500
C1C	0.6320	0.1790	0.2774	0.0304	H1F3	1.0300	0.2461	0.1161	0.0500
C3C	0.6377	0.4513	0.2601	0.0312	C1F	0.4083	0.7237	0.2979	0.0340
C2C	0.5931	0.3253	0.2926	0.0318	C6F	-0.0839	0.6383	0.7745	0.0403
H2C1	0.6026	0.3400	0.3374	0.0500	H6F	-0.0392	0.5751	0.7928	0.0500
H2C2	0.5262	0.3258	0.2806	0.0500	C3F	0.7183	0.3273	0.7801	0.0558
N1D N	0.3817	0.1697	0.8169	0.0432	H3F	0.7633	0.3904	0.7983	0.0500
H1D1	0.3279	0.1752	0.8376	0.0500	C5F	0.6451	0.0960	0.7771	0.0502
H1D2	0.3826	0.0829	0.7957	0.0500	H5F	0.6406	0.0044	0.7936	0.0500
H1D3	0.3822	0.2450	0.7886	0.0500	C4F	0.7123	0.1903	0.8037	0.0537
C1D	0.4653	0.1797	0.8630	0.0323	H4F	0.7534	0.1612	0.8375	0.0500
C6D	0.5141	0.3079	0.8703	0.0377	C2F	-0.1572	-0.1279	0.7707	0.0469
H6D	0.4941	0.3882	0.8471	0.0500	H2F	-0.1606	-0.0350	0.7862	0.0500
C4D	0.6237	0.1949	0.9474	0.0440	HO1A	0.0720	0.0589	0.9605	0.0770
H4D	0.6771	0.2000	0.9755	0.0500	HO1C	0.7425	0.0573	0.2962	0.0850
C5D	0.5938	0.3150	0.9131	0.0436	H03B	0.8963	0.4440	0.1194	0.1020
H5D	0.6269	0.4006	0.9185	0.0500	–	–	–	–	–
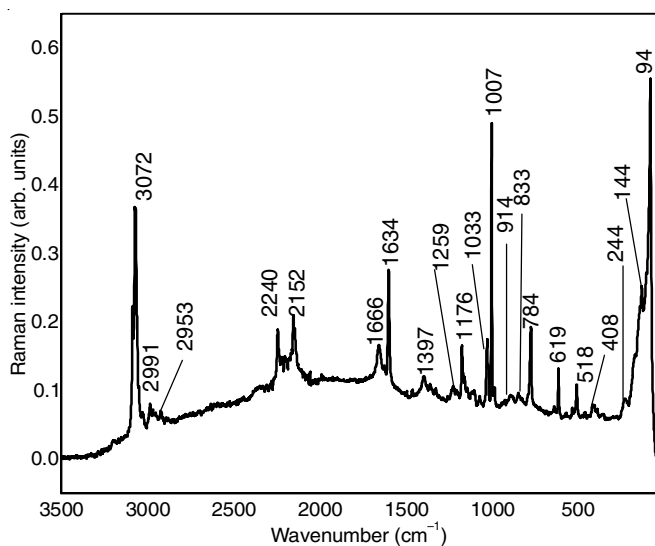
Fig. 11. FT- Raman spectra of as grown anilinium malonate crystal

Table-6. The infrared bands observed in the measured region 4000-400 cm^{-1} and Raman bands observed in the region 4000-50 cm^{-1} arise from internal vibrations of anilinium cations, malonate anions, the vibrations of hydrogen bonds and from the vibrations of lattice.

N-H vibrations: Infrared spectra of N-H stretching frequencies in the region 3100-2800 cm^{-1} and multiple combination bands in the 2900-2000 cm^{-1} which are the prominent IR bands of protonated amine salts of aniline derivatives [22]. In the region 3500- 2200 cm^{-1} there are overlapping of peaks due to O-H stretching of -COOH and N-H stretching of NH_3^+. The infrared absorption at 3197 cm^{-1} with strong intensity is assigned to NH_3^+ asymmetric stretching of anilinium cation. The broad Raman peak with weak intensity at 1634 cm^{-1} is ascribed to NH_3^+ in-plane bending vibration. The strong infrared peak at 482 cm^{-1} is attributed to NH_3^+ out-plane bending vibration [9]

C-H vibrations: NH and CH stretching frequencies are expected to occur in the higher frequency region [23]. There

TABLE-6
WAVENUMBERS (cm^{-1}) AND RELATIVE INTENSITIES OF
THE BANDS OBSERVED IN THE POWDER INFRARED AND
RAMAN SPECTRA OF THE ANILINIUM MALONATE

FT-IR	FT-Raman	Band assignment
3197s		NH$_3$ symmetric stretching
3060s	3072w	C-H stretching (benzene)
2902sb	2991vw	O-H stretching
2853s	2953w	N-H···O stretching
2732s		N-H···O stretching
2329m		O-H stretching
	2240m	O-H stretching
	2152m	O-H stretching
1961ms		COO$^-$asymmetric stretching
1678sb	1666vwb	C=O asymmetric stretching
	1634vwb	NH$_3$ in-plane bending
1584vsb		C-C stretching
1497vs		C-C stretching
1487vs		C-C stretching
1384vs		C-O, C-O-H bending
1337s	1397vwb	C-O, C-O-H bending
1261vs	1259vw	C-C-H in-plane bending
1210s		CH$_2$ wagging, C-O-H stretching
1165ssh	1176w	C-N stretching
1078ms		C-O stretching
1069ms		C-C-H in-plane bending
1028s	1033vw	O-H in-plane bending
1005s	1007vs	C-C stretch + C-C-C in plane bend
1002s		C-C stretch + C-C-C in plane bend
938w		CH$_2$ wagging, C-O-H stretching
909mb	914vwb	C-O, C-C stretching
884w		C-C-O in plane bending+ C-O stretching
835w	833vw	C-H out plane bending
787s	784w	C-N stretching
722w		C-H out plane bending
687s		C-C-C out plane bending
615w	619vw	O-H out-plane bending
603m		O-C-O in-plane bending
530w	518vw	In plane ring deformation, NH$_3$ torsion
482s		NH$_3$ out-plane bending
460m		C-N out plane bending
411m	408vw	OH bending
	244vwb	C-C-C-N torsion
	144msh	C-C-C in-plane bending vibration
119vw		O-H stretching
100vw	94ssh	O-H stretching

are multiple weak bands in the region 3100-3000 cm^{-1} due to aromatic C-H stretching vibrations in aromatic compounds [24-26] and this weak in intensity is due to the decrease of dipole moment caused by the reduction of negative charge on the carbon atoms. This reduction occurs because of the electrons withdrawing on the carbon atoms by the substituent due to the decrease of inductive effect, which in turn is caused by the increased chain length of the substituent [27]. In general, C-H in-plane and out-plane-bending vibrations are expected to be observed in the range 1300-1000 cm^{-1} and 1000-750 cm^{-1} respectively. The strong infrared peak at 1210 cm^{-1} is attributed to C-H out plane bending vibration. Medium infrared peak at 938 cm^{-1} is assigned to C-H out plane bending vibration. The weak infrared peaks 835 and 722 cm^{-1} are assigned to C-H in-plane bending vibration [28].

C-C vibrations: Two strong infrared bands at 1005 and 1002 cm^{-1} with strong Raman counterpart at 1007 cm^{-1} are

attributed to C-C stretching as well as C-C-C in-plane bending vibration of benzene ring in anilinium cation [9,29]. The ring stretching C-C-H mode of vibration in aniline usually occurs at 1306 cm^{-1}. This peak appears at 1260 cm^{-1} in infrared spectrum with strong intensity and its Raman counterpart occurs at 1259 cm^{-1} with weak intensity may be due to self-association with intermolecular interactions. The strong infrared peaks at 1584, 1497 & 1487 cm^{-1} are ascribed to C-C stretching vibration of aniline ring. The medium strong infrared peak at 1069 cm^{-1} and 687 cm^{-1} is attributed to C-C-H in-plane bending vibration and out-plane bending vibration respectively. The very weak Raman peak at 244 cm^{-1} is attributed to C-C-C-N torsional vibration [24].

C-N vibrations: It is difficult to assign C-N stretching since mixing of several bands is possible in this region. Silverstein *et al.* [30] assigned the C-N stretching absorption in the region 1382-1266 cm^{-1} for aromatic amines. Upon ionization of aniline, the C-N bond significantly shortens due to an increased conjugation between the planar NH$_2$ group and the ring. The medium infrared and Raman peak at 1165/1176 cm^{-1} is assigned to C-N stretching. The medium IR peak at 787 cm^{-1} with Raman peak at 784 cm^{-1} is assigned to C-N in-plane bending vibration whereas C-N out-of-plane bending is observed at 460 cm^{-1} in Raman spectra.

COO$^-$ and COOH vibrations: The carboxyl group of organic compounds with strong infrared absorption are usually observed in the region 1850-1650 cm^{-1}. Protonation strongly influence the intensity of carbonyl C=O stretching band in the 1735-1675 cm^{-1} region. The strong infrared peak at 1678 cm^{-1} is due to asymmetric stretching of carbonyl groups. Its corresponding Raman counterpart observed at 1666 cm^{-1} with weak intensity. Usually this peak is observed at 1730 cm^{-1}. The reduction in this frequency clearly confirm the occurence of proton transfer from the carboxylic acid to the amine molecules. In addition to that, the carboxylic group vibrations, C-O stretching, ν(C-O) and in-plane C-O-H bending are expected to appear in the range 1150-1450 cm^{-1}. The strong infrared peaks at 1384 and 1337 cm^{-1} is attributed to C-O-H bending vibration. Its Raman counterpart occurs at 1397 cm^{-1} with weak intensity. Generally, the ν(C-O) stretching occurs at higher frequencies than in-plane C-OH bending. Based on the above fact, a medium infrared peak at 1078 cm^{-1} is assigned to C-O stretching vibration of malonic acid [31,32]. The medium intensity infrared peak at 603 cm^{-1} is due to O-C-O in-plane bending vibration.

O-H vibrations: The vibrations of various carboxylic acids like malonic acid, succinic acid, adipic acid are discussed by Tarakeshwar and Manogaran [33]. Kidric *et al.* [34] investigated the intramolecular hydrogen bonding interactions in aniline hydrogen malonates. Based on the geometrical parameters of hydrogen atoms, there are 24 hydrogen bonds of N-H···O, O-H···O types cover different ranges of lengths with different average value of length. The N-H···O types cover the range of 2.7329-3.0223 Å with the average value of 2.8776 Å. The O-H···O types cover the range 2.5233-2.5836 Å with the average value equal to 2.5535 Å. The net effect of all the hydrogen bonds is to form a three dimensional network. The vibrational frequencies of N-H···O stretching occurs at 2853

and 2732 cm^{-1} in infrared spectra with strong intensity and 2953 cm^{-1} in Raman spectra with weak intensity. The OH group vibrations are more sensitive to the environment. The broad peak with strong intensity at 2902 cm^{-1} in infrared spectrum and weak intensity peak at 2991 cm^{-1} is assigned to O-H stretching. The strong IR peak at 1028 cm^{-1} and weak Raman peak at 1033 cm^{-1} is also assigned to O-H stretching of carboxyl group [24]. The infrared peak at 2329 cm^{-1} and Raman peaks at 2240 and 2152 cm^{-1} with medium intensity are assigned to O-H stretching of malonic acid. The weak IR/Raman peak at 615/619 cm^{-1} is assigned to O-H out-plane bending of malonic acid [33].

Hirshfeld surface analysis: Hirshfeld surface analysis provides the visualization of intermolecular interactions in molecular crystals [35] and used to get the 3D Hirshfeld surfaces and 2D finger plots of the obtained crystal. By taking electron distribution as a sum of spherical atom electron densities, Hirshfeld surfaces are constructed [36]. The normalized contact distance d_{norm} based on the distance from a point on the surface to the nearest nucleus outside the surface, d_e is the distance from a point on the surface to the nearest nucleus inside the surface, d_i enables the identification of the regions of particular importance to the intermolecular interactions. The intermolecular contacts in the crystal lattice is provided by the combination of d_e and d_i in the form of two-dimensional fingerprint plot [37]. CRYSTAL EXPLORER3.1 software program generates the Hirshfeld surfaces mapped with d_{norm} and two dimensional fingerprint plots [38]. The normalized
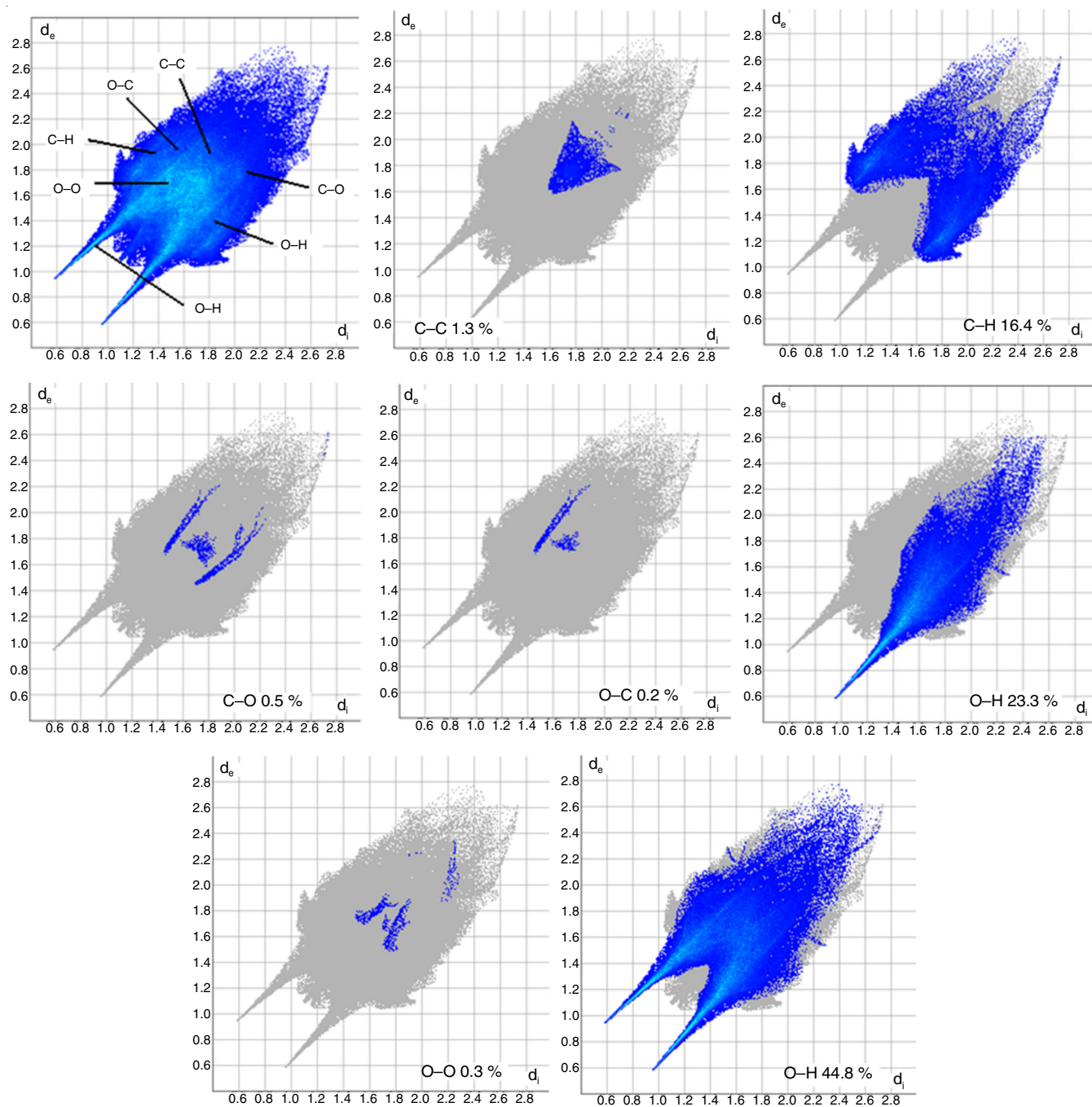
Fig. 12. Relative contributions to the percentage of Hirshfeld surface area for the various intermolecular contacts in anilinium malonate crystal
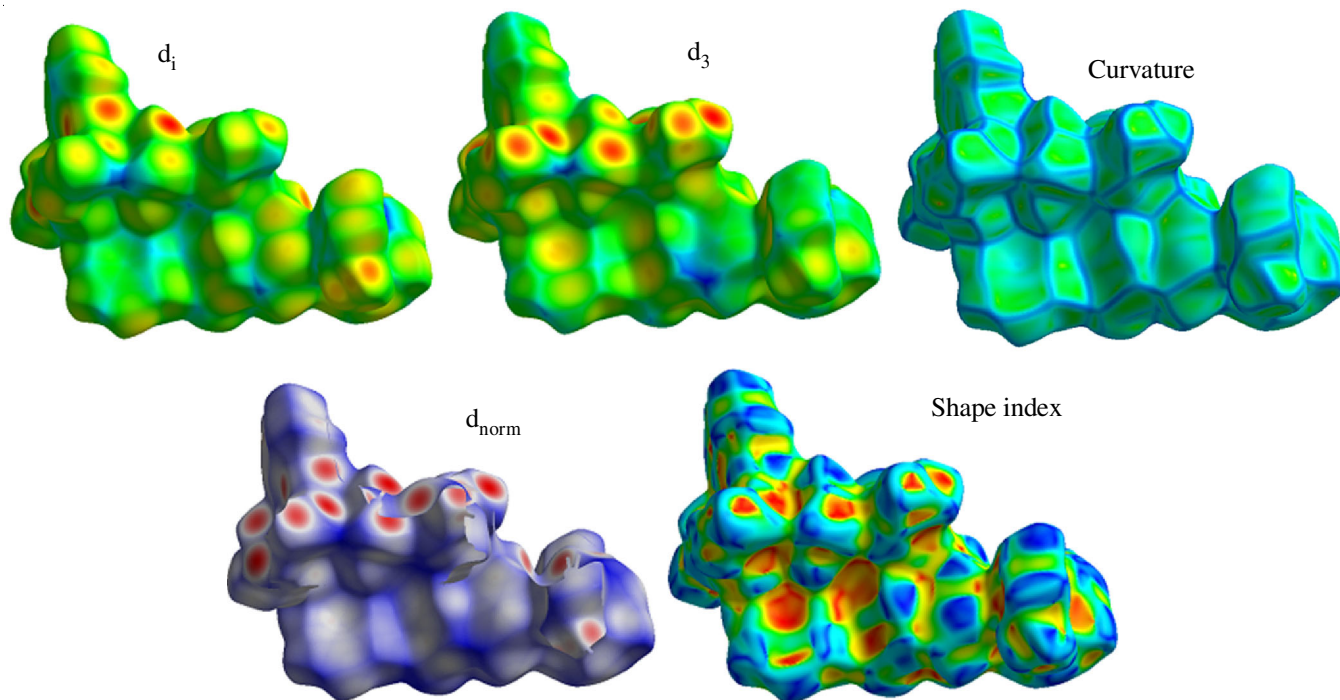
Fig. 13. Hirshfeld surface analysis d_i, d_e, d_{norm}, shape index and curvedness of anilinium malonate

contact distance $d_{norm} = d_i - r_i^{vdw}/r_i^{vdw} + d_e - r_e^{vdw}/r_e^{vdw}$ where r_i^{vdw} and r_e^{vdw} are the van der Waals radii of the atoms. The intermolecular contact is shoreter than r^{vdw} if d_{norm} is negative and longer if d_{norm} is positive. The red-white-blue colour in Hirshfeld surface map represents the shortest intermolecular contact, contact around r^{vdw} separation and longer intermolecular contact distance respectively. The 2D fingerlpot is a combination of d_e and d_i provides the summary of intermolecular contacts in the crystal and are in complement to the Hirshfeld surfaces [37]. The shape index and curvedness are the two coloured properties can also be specified based on the local curvature of the surface.

The intermolecular interactions of the title compound are quantified using Hirshfeld surface analysis. Like Fourier transform infrared spectrum, Hirshfeld surfaces also unique for a particular crystal structure. Finger print (Fig. 12) indicates the contributions of inter contacts to the Hirshfeld surfaces, C-C (1.3 %), C-H (16.4 %), C-O (0.5 %), O-C (0.2 %), O···H (23.3 %), O-O (0.3 %), O-H (44.8 %). These inter-contacts are highlighted by conventional mapping of d_{norm} on molecular Hirshfeld surfaces as shown in Fig. 12. The red spots over the surface indicate the intercontacts involved in the hydrogen bonds. Further, intercontacts are plotted with fingerprint plots. The mapping of d_i, d_e, d_{norm}, shape index and curvedness are shown in Fig. 13. d_{norm} ranges from (-0.005 to 0.000 Å); shape index ranges from (-1.00 to 1.000 Å) curvedness ranges from (-4.000 to 0.400 Å) d_e (0.590 to 2.796 Å) d_i (0.5882 to 2.756 Å).

Conclusion

Anilinium malonate crystals have been grown by slow solvent evaporation technique and crystallize in the centrosymmetric space group of monoclinic system (P2(1)/n). Single crystallographic X-ray diffraction analysis provided an under-

standing of the structural features of anilinium malonate crystal. The vibrational spectroscopic analysis elucidates the presence of various functional groups in the aniline and malonic acid crystalline product. The strong inter- and intramolecular interactions give notable vibrational effect. Further theoretically obtained powder X-ray diffraction pattern calculates the crystal size as 13.962 μm from Debye Sherrer formula. The Hirshfeld surface analysis with finger plots and electrostatic potential map shed more light on the percentage of intermolecular contacts and distribution of electrostatic potential of the title compound.

Supplementary material: Full crystallographic data (cif file) relating to the crystal structure have been deposited with Cambridge Crystallagraphic Data centre as CCDC 1875493. Copies of this information can be obtained free of charge from the Cambridge Crystallagraphic Data Centre, 12 Union Road, Cambridge CB2 1Ez. UK (Tel: +44(0) 1223 762911; email: deposit@ccdc.cam.ac.uk:http://www.ccdc.cam.ac.uk).

CONFLICT OF INTEREST

The authors declare that there is no conflict of interests regarding the publication of this article.

REFERENCES

1. D.S. Chemla and J. Zyss, Nonlinear Optical Properties of Organic Molecules and Crystals, Academic Press: New York, pp 110 (1987).
2. S. Shaji, S.M. Eappen, T.M.A. Rasheed and K.P.R. Nair, *Spectrochim. Acta A Mol. Biomol. Spectrosc.*, **60**, 351 (2004); https://doi.org/10.1016/S1386-1425(03)00233-6.
3. M. Arivazhagan, V.P. Subhasini and A. Austine, *Spectrochim. Acta A*, **86**, 205 (2012); https://doi.org/10.1016/j.saa.2011.10.026.
4. E. Kavitha and N. Sundaraganesan, *Indian J. Pure Appl. Phy.*, **48**, 20 (2010).
5. D.P. Anand, S.S. Kumar, K. Ambujam, K. Rajarajan, M.G. Mohammed and A. Sagayaraj, *Indian J. Pure Appl. Phys.*, **43**, 863 (2005).

6. D. Avci, A. Basoglu and Y. Atalay, *Z. Naturforsch. A*, **63**, 712 (2008); https://doi.org/10.1515/zna-2008-10-1115.

7. T. Tsunekawa, T. Gotoh and M. Iwamoto, *Chem. Phys. Lett.*, **166**, 353 (1990); https://doi.org/10.1016/0009-2614(90)85042-B.

8. P. Vivek, A. Suvitha and P. Murugakoothan, *Spectrochim. Acta A*, **134**, 517 (2015); https://doi.org/10.1016/j.saa.2014.05.051.

9. N. Kanagathara, M.K. Marchewka, G. Anbalagan, A. Ben Ahmed and H. Feki, *J. Optoelectron. Adv. Mater.*, **19**, 251 (2017).

10. E. Sapina, E. Escriva, J.V. Folgado, A. Beltran, D. Beltran, A. Fuertes and M. Drillon, *Inorg. Chem.*, **31**, 3851 (1992); https://doi.org/10.1021/ic00044a031.

11. E. Colacio, J.M. Dominguez-Vera, J.P. Costes, R. Kivekas, J.P. Laurent, J. Ruiz and M. Sundberg, *Inorg. Chem.*, **31**, 774 (1992); https://doi.org/10.1021/ic00031a016.

12. F.S. Delgado, M. Hernández-Molina, J. Sanchiz, C. Ruiz-Pérez, Y. Rodríguez-Martín, T. López, F. Lloret and M. Julve, *CrystEngComm*, **6**, 106 (2004); https://doi.org/10.1039/B403640A.

13. Q.-Z. Zhang, W.-B. Yang, S.-M. Chen and C.-Z. Lu, *Bull. Korean Chem. Soc.*, **26**, 1631 (2005); https://doi.org/10.5012/bkcs.2005.26.10.1631.

14. C. Oldham, in: G. Wilkinson, R.D. Gillard, J.A. McCleverty (Eds.), Comprehensive Coordination Chemistry, vol. 2, Pergamon Press, Oxford, 1987, 435.

15. S.-M. Zhu, *Acta Cryst.*, **E68**, o2597 (2012).

16. O. Kaman, L. Smrcok, R. Gyepes, D. Havlýcek, *Acta Cryst.*, **C68**, o57 (2012).

17. K. Diffraction, KM4/CCD Users' Guide, Version 1.169 (Release April, 2000), Wroclaw, Poland, 2000.

18. G.M. Sheldrick, X.L.SHEL, Program for Crystal Structure Refinement, University of Gottingen, Germany, 1993.

19. G.M. Sheldrick, *Acta Crystallogr. A*, **64**, 112 (2008); https://doi.org/10.1107/S0108767307043930.

20. J.A. Paixâo, A. Matos Beja, M. Ramos Silva and L. Alte da Veiga, *Z. Kristallogr. NCS*, **214**, 85 (1999).

21. C.F. Macrae, P.R. Edgington, P. McCabe, E. Pidcock, G.P. Shields, R. Taylor, M. Towler and J. van de Streek, *J. Appl. Cryst.*, **39**, 453 (2006); https://doi.org/10.1107/S002188980600731X.

22. R.M. Siverstein and F.X. Webster, Spectrometric Identification of Organic Compounds, Sixth Ed., Wiley 1998, Chapter 3, pp. 102.

23. M. Drozd and M.K. Marchewka, *J. Mol. Struct. THEOCHEM*, **716**, 175 (2005); https://doi.org/10.1016/j.theochem.2004.11.020.

24. N. Kanagathara, M.K. Marchewka, M. Drozd, S. Gunasekaran, P.R. Rajakumar and G. Anbalagan, *Spectrochim. Acta A*, **145**, 394 (2015); https://doi.org/10.1016/j.saa.2015.03.002.

25. A. Poiyamozhi, N. Sundaraganesan, M. Karabacak, O. Tanrýverdi and M. Kurt, *J. Mol. Struct.*, **1024**, 1 (2012); https://doi.org/10.1016/j.molstruc.2012.05.008.

26. V. Krishnakumar, V. Balachandran and T. Chithambarathanu, *Spectrochim. Acta A*, **62**, 918 (2005); https://doi.org/10.1016/j.saa.2005.02.051.

27. H. Spedding and D.H. Whiffen, *Proc. R. Soc. Lond. A Math. Phys. Sci.*, **238**, 245 (1956).

28. D.N. Sathyanarayana, Vibrational Spectroscopy, Theory and Applications, New Age International (P) Ltd. Publishers: New Delhi (1996).

29. M.K. Marchewka, S. Debrus, M. Drozd, J. Baran, A.J. Barnes, D. Xue and H. Ratajczak, *Pol. J. Chem.*, **77**, 1625 (2003).

30. R.M. Silverstein, G.C. Bassler and T.C. Morril, Spectrophotometric Identification of Organic Compounds (1981) John Wiley and Sons, New York.

31. K.C. Russell, J.-M. Lehn, N. Kyritsakas, A. DeCian and J. Fischer, *New J. Chem.*, **22**, 123 (1998); https://doi.org/10.1039/a708318a.

32. R.F.M. Lange and E.W. Meijer, *Macromol. Symp.*, **102**, 301 (1996); https://doi.org/10.1002/masy.19961020136.

33. P. Tarakeshwar and S. Manogaran, *J. Mol. Struct. THEOCHEM*, **362**, 77 (1996); https://doi.org/10.1016/0166-1280(95)04375-6.

34. J. Kidriè, J. Mavri, M. Podobnik and D. Had•i, *J. Mol. Struct.*, **237**, 265 (1990); https://doi.org/10.1016/0022-2860(90)80144-9.

35. M.J. Turner, J.J. McKinnon, S.K. Wolff, D.J. Grimwood, P.R. Spackman, D. Jayatilaka and M.A. Spackman, CrystalExplorer17 (2017). University of Western Australia. http://hirshfeldsurface.net.

36. M.A. Spackman, J.J. McKinnon and D. Jayatilaka, *CrystEngComm*, **10**, 377 (2008).

37. M.A. Spackman and J.J. McKinnon, *CrystEngComm*, **4**, 378 (2002); https://doi.org/10.1039/B203191B.

38. S. K. Wolff, D. J. Greenwood, J. J. McKinnon, M. J. Turner, D. Jayatilaka, M. A. Spackman. (2012) Crystal Explorer, Version 3.1.